Towards the Maximization of Renewable Energy Integration Using a Stochastic AC-QP Optimal Power Flow Algorithm

Jennifer F. Marley
Valparaiso University

Maria Vrakopoulou
ETH Zürich, Switzerland

Ian A. Hiskens
University of Michigan

***Abstract*—Renewable generation sources are becoming more critical to the economic and environmental operation of power systems. Maximizing the renewable generation in a network is therefore an important planning problem. Such problems must consider the stochastic nature of the energy sources in order to maintain reliability standards. Moreover, accurate methods for representing the non-convex network power flow equations should be utilized in order to obtain reliable solutions. This paper provides a stochastic AC optimal power flow (OPF) formulation that maximizes the total wind generation in the system. The approach utilizes an AC OPF method that is based on successive quadratic programming (AC-QP) and scenario-based optimization to deal with stochasticity. In doing so, the resulting AC-feasible solution is accompanied by theoretical a-posteriori reliability guarantees. The performance of the proposed algorithm is assessed in terms of optimality, solution time, and empirical and a-posteriori theoretical probabilities of violation.**

***Index Terms*—AC optimal power flow, integration of renewable generation, forecast uncertainty, scenario-based optimization.**

I. INTRODUCTION

Sustainable operation of power systems is dependent upon increased penetration of renewable generation. However, such generation presents reliability challenges due to its inherent variability. Given a set of potential wind locations within a network, determining the maximum wind capacity that could be installed at those locations is an important planning problem. Solution methods have been developed for this problem but they typically make use of a DC power flow approximation [1]. There remains a need for a solution methodology that accommodates the complexities introduced by both generation uncertainty and AC power flow feasibility.

The goal of any optimal power flow (OPF) problem is to optimize a certain objective (e.g. minimization of generation cost or minimization of power losses), while satisfying a set of operational and engineering constraints (e.g. generator and line flow limits). The AC OPF is a particularly challenging problem, due to the non-convex nature of the AC power flow equations. Many solution methods have been developed for this problem. A common approach is to use the DC power flow approximation to cast the problem as a quadratic program (QP) [2],[3]. Such formulations are highly scalable, as reliable solvers have been developed for large-scale QPs. However, accuracy may be an issue [4]. Recent work has focused on developing convex relaxations of the OPF problem to form semidefinite (SDP) and second-order cone programs (SOCP) [5], [6]. While these relaxations provide globally optimal solutions when tight, their tightness cannot be guaranteed for arbitrary networks [7],[8]. Moreover, the scalability of such formulations is limited by currently available solvers.

The AC-QP OPF algorithm [9] is a successive linearization solution method that alternates between solving a simple QP and running a full AC power flow. This method provides an AC-feasible solution and is highly scalable with respect to network size. However, the algorithm may provide only locally optimal solutions and may not always converge. Subsequent work will be based in the AC-QP OPF method as it provides an AC-feasible solution and scales better than convex relaxation approaches.

A stochastic OPF is required to deal with the variability inherent in wind power generation. Several stochastic OPF formulations have been developed using DC power flow approximations [10], [11], [12], [13], [14], [15]. However, increased accuracy in modeling the network is crucial to maintaining reliability standards. To incorporate uncertainty into the problem, some approaches heuristically choose a set of scenarios to include in the OPF [10], [11], [12], possibly also using a scenario reduction technique. However, such methods do not provide any probabilistic guarantees of the solution. Alternatively, if a closed form of the uncertainty distribution is assumed, the problem can be analytically reformulated [14], [15]. However, extending these reformulations to non-convex OPF problems is not necessarily straightforward, and the assumption of a particular uncertainty distribution may be inaccurate. Robust optimization techniques have also been developed [16], but may provide solutions that are overly

This work was supported by the National Science Foundation through grants CNS-1238962 and CCF-1442495, and by the European Research Council under the European Unions Seventh Framework Programme (PIOF-GA-2013-626014).

J. Marley is with the Department of Electrical and Computer Engineering, Valparaiso University, Valparaiso, IN 46383, USA. Email: jkfelder@umich.edu.

M. Vrakopoulou is with the Department of Information Technology and Electrical Engineering, ETH Zürich, Switzerland. Email: vrakopoulou@control.ee.ethz.ch

I. Hiskens are with the Department of Electrical Engineering and Computer Science, University of Michigan, Ann Arbor, MI 48109, USA. Email: hiskens@umich.edu.

conservative, depending on the chosen uncertainty set.

Another class of methods follow from so-called scenario-based optimization. Approaches such as [17], [18], [19] provide a-priori performance guarantees and do not assume a specific uncertainty distribution. These approaches were first applied to the stochastic DC OPF problem in [13] and later to the SDP relaxation of the stochastic AC OPF in [20]. As the AC OPF problem is non-convex, the methods in [17], [18] cannot be directly applied, as they require the underlying problem to be convex. Moreover, because it is not straightforward to find the optimal solution of a robust counterpart of the initial problem, the method [19] is not applicable in the AC-QP setting.

This paper utilizes a scenario-based optimization technique that offers a-posteriori performance guarantees for non-convex problems [21]. This result was initially used in an OPF context in [22]. It will be extended to the problem of maximizing wind power integration, and will make use of the AC-QP OPF to obtain good scalability properties.

The remainder of the paper is organized as follows. Section II describes the AC-QP OPF solution method for determining the maximum wind generation that can be integrated in a network. This formulation is then extended to a stochastic OPF formulation in Section III. The stochastic OPF problem is accompanied by a-posteriori theoretical guarantees on the probability of violation, which are developed in Section IV. Results for the IEEE 118-bus network are provided in Section V, and conclusions are offered in Section VI.

II. Deterministic Maximization of Wind Power

The AC quadratic program OPF (AC-QP OPF) algorithm used in this work is based on the method described in [9]. It is a successive linearization method that begins by solving an AC power flow from an initial operating point. The solution of this power flow is used to linearize the non-convex line flow and power balance constraints, approximating the AC OPF as a QP. The solution of this QP provides a new dispatch to run the next AC power flow. These iterations continue until the QP and power flow solutions agree within a small tolerance (10^{-3} p.u. provides sufficient accuracy). This algorithm is summarized in Figure 1.

An SOCP relaxation based on the formulation in [5] is solved to provide an initialization for this method. The relaxation provides initial schedules for generator active and reactive power output, as well as the voltage magnitude at each bus in the network. This procedure has been demonstrated to improve the convergence and optimality of the local AC-QP solution method [23]. To further improve the convergence of this algorithm, a trust region method based on the approach in [24] is included. By restricting the magnitude of changes that can be scheduled by the QP at each iteration of the AC-QP algorithm, this step improves the accuracy of the linearization used in the power balance and line flow constraints. A detailed discussion of this step is provided in [23].

This method is used to solve an AC OPF problem with the modified objective of maximizing the amount of wind generation added to the network of interest. As such, the proposed formulation is applicable in a planning context, where deciding the amount of wind that can be installed at predetermined locations is an important problem. In the formulation that follows, the superscript '∘' denotes values obtained from the previous AC power flow solution. These are fixed parameters in the QP, and are updated after each AC power flow to relinearize the network constraints. The notation Δ denotes a change from the converged power flow solution of the corresponding variable at the current iteration of the AC-QP algorithm. These are the decision variables in the QP. Table I summarizes the notation in the problems that follow.

TABLE I
Notation.

Decision Variables:	
$\Delta P_{g,i}$	change in active power generation at node $i \in \mathcal{G}$
$\Delta P_{w,i}$	change in base case wind forecast at node $i \in \mathcal{W}$
$\Delta Q_{g,i}$	change in reactive power generation at node $i \in \mathcal{G}$
d	participation vector of generators
ΔV_i, $\Delta\theta_i$	change in voltage magnitude, angle at node $i \in \mathcal{N}$
$\Delta Q^m_{g,i}$	change in reactive power generation at node $i \in \mathcal{G}$ in scenario $m \in \mathcal{S}$
ΔV^m_i, $\Delta\theta^m_i$	change in voltage magnitude, angle at node $i \in \mathcal{N}$ in scenario $m \in \mathcal{S}$
Parameters :	
$\mathcal{G}$	set of conventional generation nodes
$\mathcal{W}$	set of wind nodes
$\mathcal{S}$	set of wind power scenarios
$\mathcal{N}$	set of nodes in the network
$\mathcal{L}^*$	set of lines at or above 95% of their limit
$slack$	slack node in the network
S^{max}_{ij}	maximum apparent power flow in line from node i to node j
$P^{min}_{g,i}, P^{max}_{g,i}$	minimum, maximum active power limits when generator at node $i \in \mathcal{G}$ is in service
$P^{max}_{w,i}$	maximum active power limit for wind generator at node $i \in \mathcal{W}$
$Q^{min}_{g,i}, Q^{max}_{g,i}$	minimum, maximum reactive power limits when generator at node $i \in \mathcal{G}$ is in service
$\frac{\partial S_{ij}}{\partial\theta_k}, \frac{\partial S_{ij}}{\partial V_k}$	AC line flow sensitivity factors
$\mathbf{J}$	AC power flow Jacobian matrix
V^{min}_i, V^{max}_i	minimum, maximum voltage magnitude at node $i \in \mathcal{N}$
G_a	node-generator incidence matrix
W_a	node-wind incidence matrix
E^m_i	percentage of nominal wind generation for node i in scenario m

The QP solved at each iteration is then formulated as:

$$\max \sum_{i\in\mathcal{W}} \left(P^\circ_{w,i} + \Delta P_{w,i}\right) \tag{1a}$$

subject to

$$\mathbf{J}\Delta x = \Delta S \tag{1b}$$

$$P^{min}_{g,i} \leq P^\circ_{g,i} + \Delta P_{g,i} \leq P^{max}_{g,i} \qquad \forall i \in \mathcal{G} \tag{1c}$$

$$Q^{min}_{g,i} \leq Q^\circ_{g,i} + \Delta Q_{g,i} \leq Q^{max}_{g,i} \qquad \forall i \in \mathcal{G} \tag{1d}$$

$$0 \leq P^\circ_{w,i} + \Delta P_{w,i} \leq P^{max}_{w,i} \qquad \forall i \in \mathcal{W} \tag{1e}$$

$$\Delta\theta_{slack} = 0 \tag{1f}$$

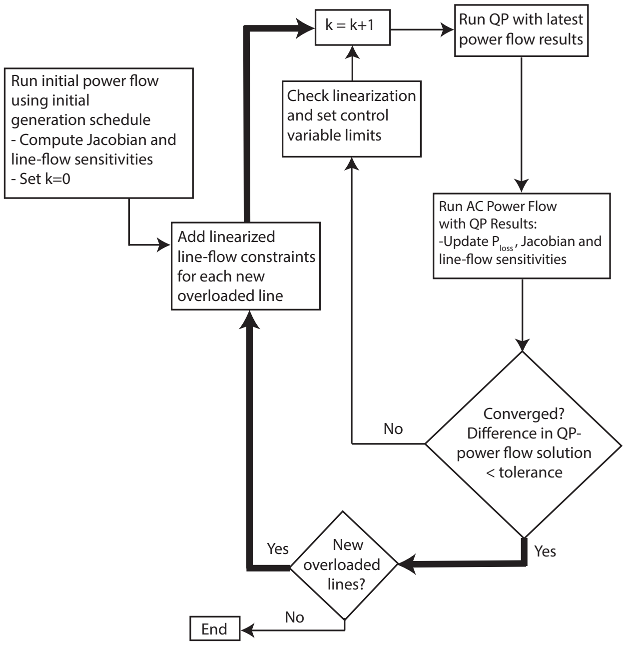

Fig. 1. AC-QP OPF algorithm.

$$V_i^{min} \leq V_i^{\circ} + \Delta V_i \leq V_i^{max} \qquad \forall i \in \mathcal{N} \tag{1g}$$

$$S_{ij}^{\circ} + \sum_{k\in\mathcal{N}} \frac{\partial S_{ij}}{\partial \theta_k}^{\circ} \Delta\theta_k + \sum_{k\in\mathcal{N}} \frac{\partial S_{ij}}{\partial V_k}^{\circ} \Delta V_k \leq S_{ij}^{max}$$
$$\forall\, (i,j) \in \mathcal{L}^* \text{ and } \forall\, (j,i) \in \mathcal{L}^* \tag{1h}$$

where

$$\mathbf{J} = \begin{bmatrix} \frac{\partial P}{\partial \theta} & \frac{\partial P}{\partial V} \\ \frac{\partial Q}{\partial \theta} & \frac{\partial Q}{\partial V} \end{bmatrix}, \Delta x = \begin{bmatrix} \Delta\theta \\ \Delta V \end{bmatrix}, \Delta S = \begin{bmatrix} G_a \Delta P_g + W_a \Delta P_w \\ G_a \Delta Q_g \end{bmatrix}.$$

The OPF objective is to maximize the total wind generation installed in the network, $\sum_{i\in\mathcal{W}}(P_{w,i}^{\circ} + \Delta P_{w,i})$. The non-convex power balance and line flow constraints are linearized through constraints (1b) and (1h) respectively. Generator active and reactive power limits are enforced in constraints (1c), (1d). The lower bound of constraint (1e) ensures the feasibility of the wind generation schedule, while the corresponding upper limit ensures that this schedule is reflective of available technology. A value of $P_{w,i}^{max} = 250$ MW was used for all studies. Bus voltage magnitude limits are enforced in (1g). Finally, the solution is restricted to a finite solution space by fixing the reference angle in constraint (1f).

Note that the linearized line-flow constraints (1h) are initially enforced for all lines that are at or above 95% of their line-flow limit, the set of which is denoted by $\mathcal{L}^*$. This set is then updated at the beginning of each outer loop of the AC-QP algorithm to include any lines that are overloaded but are not yet in the set (bolded in Figure 1). This procedure limits the number of equality constraints that must be explicitly modeled in the QP. This substantially improves the AC-QP solution time, particularly for large networks [23].

III. Scenario-Based Wind Power Maximization

A. Formulation

While the method in Section II provides an AC-feasible solution for a particular wind generation schedule (forecast), it does not take into account the stochasticity inherent in such intermittent generation sources. The deterministic method is extended to a probabilistic OPF (pOPF) framework by introducing a finite set of possible wind scenarios. As the base case wind forecast is a decision variable in this problem, a scenario is modeled as a percentage of nominal rating and is represented by the parameter E^m, where the variable $m \in \mathcal{S}$ is used to index a particular wind scenario within the set of scenarios $\mathcal{S}$. Each entry of this vector, $E_i^m \geq 0$, then gives the percentage of the base case wind generation taken at node i in scenario m. For example, $E_i^m = 0.9$ implies that for scenario m, the actual wind output at node i is 90% of the base case value.

Conventional generators must have sufficient capacity to compensate for the forecast error of each scenario $m \in \mathcal{S}$. In this work, a linear policy is adopted to respond to the generation-load mismatch introduced by these scenarios, as in [13], [9]. A distribution (or participation) vector, denoted by d and satisfying,

$$d_i \geq 0 \quad \forall i \in \mathcal{G}, \qquad \sum_{i\in\mathcal{G}} d_i = 1, \tag{2}$$

describes each generator's response to alleviating the mismatch. The base case dispatch P_g is adjusted according to the linear policy

$$P_g^m = P_g - d \sum_{k\in\mathcal{W}} (E_k^m - 1) P_{w,k} \tag{3}$$

for each scenario $m \in \mathcal{S}$. Note that in the context of maximizing the total wind added in the network, the participation vector d will also be a decision variable.

Given the set of scenarios $\mathcal{S}$ to be included in the optimization problem, the following constraints (similar to those for the base case description (1b)-(1h)) are added to the QP:

$$\mathbf{J^m} \Delta x^m = \Delta S^m \tag{4a}$$

$$P_{g,i}^{min} \leq P_{g,i}^{\circ,m} + \Delta P_{g,i} + \alpha^m d_i + d_i^{\circ} \sum_{k\in\mathcal{W}} (E_k^m - 1) P_{w,k}^{\circ}$$
$$- d_i \sum_{k\in\mathcal{W}} (E_k^m - 1)(P_{w,k}^{\circ} + \Delta P_{w,k}) \leq P_{g,i}^{max} \quad \forall i \in \mathcal{G} \tag{4b}$$

$$Q_{g,i}^{min} \leq Q_{g,i}^{\circ,m} + \Delta Q_{g,i}^m \leq Q_{g,i}^{max} \qquad \forall i \in \mathcal{G} \tag{4c}$$

$$\Delta\theta_{slack}^m = 0 \tag{4d}$$

$$V_i^{min} \leq V_i^{\circ,m} + \Delta V_i^m \leq V_i^{max} \qquad \forall i \in \mathcal{N} \tag{4e}$$

$$\Delta V_i = \Delta V_i^m \qquad \forall i \in \mathcal{G} \tag{4f}$$

$$S_{ij}^{\circ,m} + \sum_{k\in\mathcal{N}} \frac{\partial S_{ij}}{\partial \theta_k}^{\circ,m} \Delta\theta_k^m + \sum_{k\in\mathcal{N}} \frac{\partial S_{ij}}{\partial V_k}^{\circ,m} \Delta V_k^m \leq S_{ij}^{max}$$
$$\forall\, (i,j) \in \mathcal{L}^{*,m} \text{ and } \forall\, (j,i) \in \mathcal{L}^{*,m} \tag{4g}$$

where $P_g^{\circ,m}$ and $Q_g^{\circ,m}$ are the generator active and reactive power from the previous AC power flow for scenario m. The linearization for each scenario is then modeled as,

$$\Delta x^m = \begin{bmatrix} \Delta\theta^m \\ \Delta V^m \end{bmatrix},$$

$$\Delta S^m = \begin{bmatrix} G_a\Big(\Delta P_g + \alpha^m d + d^\circ \sum_{k\in\mathcal{W}}(E_k^m - 1)P_{w,k}^\circ \\ -d\sum_{k\in\mathcal{W}}(E_k^m - 1)(P_{w,k}^\circ + \Delta P_{w,k})\Big) \\ +W_a\Big(\mathrm{diag}\{E^m\}\Delta P_w\Big) \\ \\ G_a \Delta Q_g^m \end{bmatrix}.$$

In this linearization, the active power component of ΔS^m has several terms. Applying the distributed slack formulation, the term $\alpha^m d$ introduces a degree of freedom to account for the fact that active power losses differ between the base case and each scenario. It should be noted that the decision variable α^m approaches zero at convergence of the AC-QP method. The conventional generator participation in the wind-induced mismatch of scenario m is modeled by $d\sum_{k\in\mathcal{W}}[(E_k^m - 1)(P_{w,k}^\circ + \Delta P_{w,k})]$. This term is an update of the equivalent term $d^\circ \sum_{k\in\mathcal{W}}(E_k^m - 1)P_{w,k}^\circ$ computed at the previous QP-(power flow) iteration. The linearization requires the difference between these terms.

Each scenario m requires extra variables for the reactive power output of each generator ΔQ_g^m and the voltage at each bus ΔV^m, $\Delta\theta^m$. Note that both the deviation of the active power generation ΔP_g and the generator voltage magnitude setpoints are required to take the same value for the base case and all scenarios. The latter requirement is enforced by the constraint (4f).

The algorithm provides a solution satisfying the non-convex AC power flow constraints for the base case and all considered scenarios. However, there is no guarantee that the solution will be feasible for any arbitrary wind scenario. A randomized optimization technique, presented in Section IV, is employed to provide such guarantees.

B. Addressing the bilinearity in the AC-QP pOPF problem

As P_w, α^m, and d are all decision variables in the pOPF problem, bilinearities arise in the terms of constraints (4a) and (4b) that contain products of these variables. These bilinear terms are solved by replacing the QP with a two-stage iterative solution method, the details of which are summarized in Figure 2.

The objective of the first stage is to determine the maximum base case wind generation that can be added in the network, subject to the linearized network constraints. The QP is solved assuming that the vector d is a fixed parameter, while α^m and ΔP_w are decision variables. The values of α^m and ΔP_w determined in Stage 1 are then fixed in Stage 2, where an optimal value of d is determined. In Stage 2, the original objective of maximizing total wind generation (which is a fixed parameter in this stage) is replaced by the modified objective of maximizing total reserve capacity of all conventional generators, modeled as,

$$\max \sum_{i\in\mathcal{G}} \Big((P_{g,i}^{max} - P_{g,i}^\circ - \Delta P_{g,i}) + (P_{g,i}^\circ + \Delta P_{g,i} - P_{g,i}^{min}) \Big). \quad (5)$$

The intuition behind this modified objective is that if conventional generators have larger reserve capacity, more wind can be integrated into the network in the next stage, as generators have greater ability to respond to larger forecast errors. This is a consequence of the linear policy assumed for the response of conventional generators to wind generation forecast errors. Stage 2 provides an updated value of the vector d to Stage 1. These iterations repeat until the change in the total base case wind forecast, $\sum_{i\in\mathcal{W}}(P_{w,i}^\circ + \Delta P_{w,i})$, is within a small tolerance. Figure 2 provides a summary. This iterative solution process replaces the "Run QP with latest power flow results" box in Figure 1.

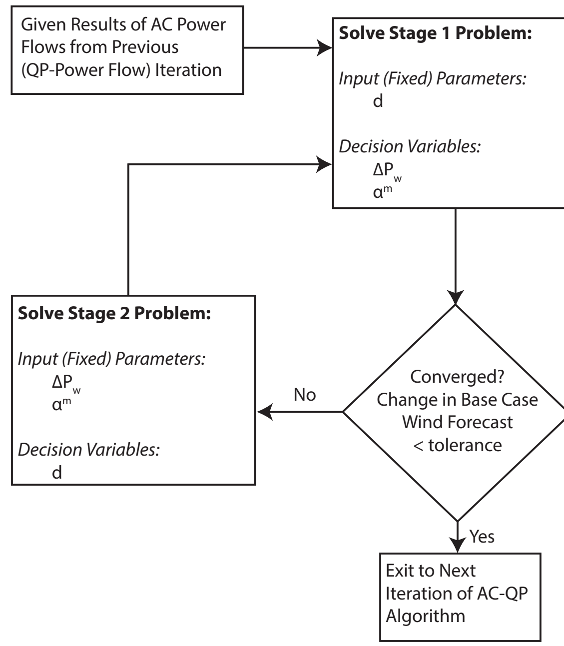

Fig. 2. Iterative solution algorithm for bilinear terms in constraints (4a) and (4b).

C. Improving the scalability of the AC-QP pOPF algorithm

The scalability of the proposed method, in terms of the number of scenarios considered, is a major advantage of the AC-QP pOPF formulation compared to other methods of solving AC OPF problems, such as convex relaxations. To achieve scalability of the method, an iterative procedure for introducing scenarios into the pOPF problem is summarized in Figure 3. This approach is based on ranking the scenarios according to two criteria. Initially, scenarios are ranked according to the difference between the scenario and the forecast, $\sum_{i\in\mathcal{W}}(P_{w,i}^m - P_{w,i})$. Only the highest and lowest ranked wind scenarios are explicitly included in the pOPF problem. These are the scenarios introducing the most positive and most negative generation-load mismatch. If the resulting solution of the AC-QP pOPF has constraint violations for any of the remaining $(N-2)$ scenarios, the scenario that has the largest number of constraint violations is then added at the next iteration. In practice, it has been observed that only a small number of scenarios must be explicitly modeled in the optimization in order to satisfy the constraints for a very large number of scenarios.

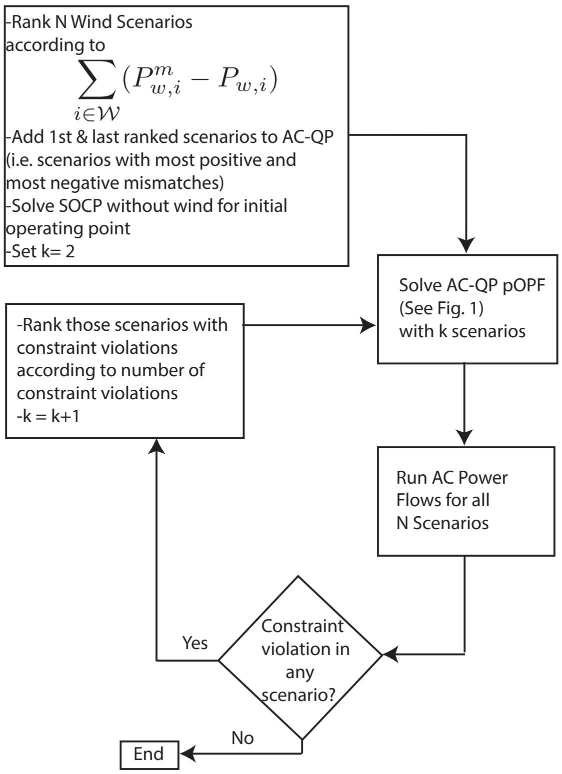

Fig. 3. AC-QP pOPF algorithm for N scenarios. The QP solved at each iteration focuses on wind power maximization.

IV. Providing a-posteriori probabilistic guarantees

The algorithm proposed in Section III-C provides a method for selecting a subset of scenarios to include in the pOPF problem to generate a solution that is feasible for a much larger set of scenarios. As such, the solution resulting from optimizing over a very small number of scenarios is an identical feasible solution to the pOPF problem where the entire (potentially much larger) set of scenarios is considered. The fact that the solution satisfies the constraints for all other scenarios, even though they were not used explicitly in the solution method, is a crucial property of this algorithm [25].

The framework in [21] is then employed to find a-posteriori probabilistic guarantees to accompany the solution of this non-convex problem. This result is applicable to any algorithm that takes as input a particular set of scenarios and provides a feasible solution to the problem. The critical point is the definition of the support set, also known as a compression scheme in [25]. Consider the solution of the problem obtained using a set of N scenarios $\mathcal{S}_N$. If the identical solution is obtained using a subset $\mathcal{S}_k$ of $\mathcal{S}_N$ that contains only k scenarios, the set $\mathcal{S}_k$ is a support set of the problem with N scenarios. In other words, the set of scenarios $\mathcal{S}_k$ supports the solution.

Having identified the cardinality k of the support set of the problem associated with N scenarios, a theoretical upper bound on the probability of constraint violation is provided by the formula from [21]:

$$\epsilon(k) = \begin{cases} 1, & \text{if } k = N \\ 1 - \sqrt[N-k]{\frac{\beta}{N\binom{N}{k}}}, & \text{otherwise} \end{cases} \tag{6}$$

where $\beta \in (0,1)$ is a design parameter representing the probability that the upper bound ϵ will be violated. In other words, β is the probability that the probability of constraint violation will be greater that ϵ. A choice of β that is sufficiently small (e.g. $\beta = 10^{-4}$) ensures that the bound ϵ will be true with "very high confidence".

It is important to note that there are only two assumptions required for this bound to be valid. First, the algorithm must map the scenario set to a 'unique' solution satisfying the constraints for all the scenarios in the set. Second, the solution must be invariant to any permutation of the scenarios. Both these requirements are satisfied for the proposed algorithm.

The provided theoretical guarantees are a-posteriori, as the cardinality of the support set can only be identified after the solution is obtained. Moreover, the result will be less conservative if a support set of minimum cardinality is found.

V. Results and Discussion

The proposed method was tested on the IEEE 118-bus network [26] that has been augmented with 10 randomly chosen wind nodes. It was assumed that each potential wind site has a maximum capacity of 250 MW. The results of this test case for an increasing number of scenarios (i.e. the value of N in Figure 3) are summarized in Figures 4 to 8. Boxplots are used to summarize the results of 500 repeated trials, where each trial differs in the specific set of N randomly chosen wind scenarios. These give several statistical quantities of interest for each set of 500 trials: the central line inside the box shows the median over all 500 trials; the bottom and top edges of each box show the 25% and 75% percentiles respectively; and the vertical lines extend to the most extreme values that are not considered statistical outliers. Those outliers are marked by an asterisk.

Figure 4 shows the amount of wind that can be added in the network for various sets of N scenarios. These results demonstrate the need to account for the uncertainty of wind generation when planning how much wind to install at various network locations. If only 100 scenarios are considered, the median total wind generation added to the network is 1713 MW. However, the median total wind generation decreases to 1138 MW when 1500 scenarios are included in the optimization. Increasing the number of scenarios implies greater wind variability, and hence a wider range of operating conditions. Consequently, less wind can be added to the network.

The scalability of the proposed method is highlighted by the results in Figure 5. In all trials (other than outliers), the AC-QP pOPF algorithm solved within 18 minutes (1080 seconds), which is an appropriate time frame for planning problems. It should also be noted that the median times are less than

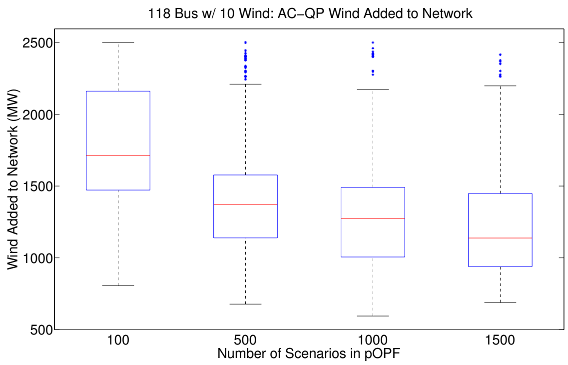

Fig. 4. AC-QP wind added to network.

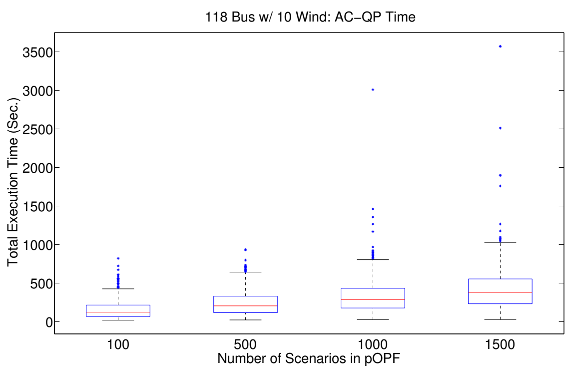

Fig. 5. AC-QP total execution time.

500 seconds (8 minutes). Moreover, due to the iterative manner in which scenarios are introduced into the problem, the execution time is only slightly affected by increasing N in the pOPF problem. Thus, the method is scalable with respect to network size and to the number of scenarios for which the resulting solution must be feasible.

Figure 6 shows the cardinality of the set of support scenarios identified in each trial. Denoted k in (6), this number is used to calculate the theoretical a-posteriori probability of violation for each trial (shown in Figure 7). While the number of support scenarios increases as does the number of scenarios considered in the problem, they remain a very small fraction of the sufficiently large sets of N scenarios. This translates into reasonably low theoretical upper bounds on the probability of violation. As Figure 7 shows, the support set results correspond to theoretical upper bounds ranging from 20-33% when only 100 scenarios are considered to less than 10% when N is increased to 1000 scenarios.

The empirical quality of solutions from the AC-QP pOPF algorithm is assessed via Monte Carlo simulations using 10,000 possible scenarios. For each scenario, an AC power flow is run and the violation of any constraint is checked. Out of those 10,000 scenarios, those that result in any constraint violations (including generator active and reactive power limits, voltage magnitude limits, and line flow limits) are recorded to provide an empirical probability of constraint violation. The results

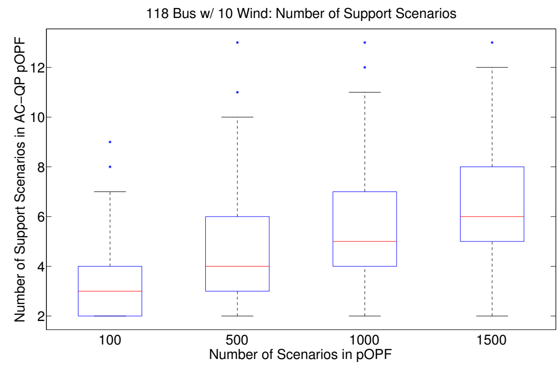

Fig. 6. AC-QP number of support scenarios.

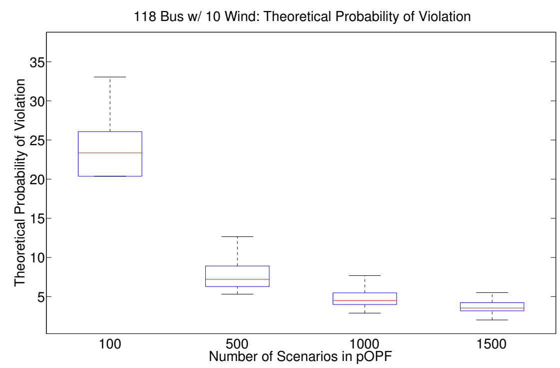

Fig. 7. AC-QP a-posteriori theoretical probability of violation.

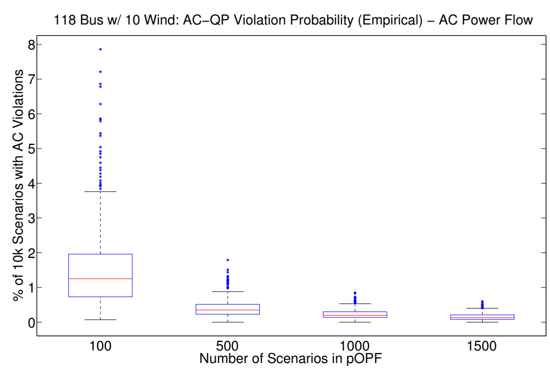

Fig. 8. AC-QP empirical probability of violation.

of these simulations are summarized in Figure 8. While the theoretical upper bound on the probability of violation is unacceptably high for the case of $N = 100$, the empirical results are much more reasonable. In this case, the empirical probability of violation is below 10% for all trials, and is less than 1% when N is increased to at least 1000 scenarios.

VI. Conclusions

The stochastic AC-QP pOPF algorithm has been extended to a planning context to determine the maximum wind penetration that can be integrated in a network while maintaining reliability standards. The scalability of this method with respect to large numbers of wind scenarios and moderate network size has been demonstrated. The proposed algorithm does not rely upon model approximations and provides an AC-feasible solution, ensuring reliable guidance for wind installation. Moreover, through the application of the scenario approach from the field of randomized optimization, the final solution is accompanied with theoretical a-posteriori guarantees on the probability of constraint violation.

REFERENCES

[1] M. Vrakopoulou, S. Chatzivasileiadis, E. Iggland, M. Imhof, T. Krause, O. Makela, J. L. Mathieu, L. Roald, R. Wiget, and G. Andersson, "A unified analysis of security-constrained OPF formulations considering uncertainty, risk, and controllability in single and multi-area systems," in *IREP Symposium Bulk Power System Dynamics and Control - IX Optimization, Security and Control of the Emerging Power Grid*, 2013.

[2] A. Motto, F. Galiana, A. Conejo, and J. Arroyo, "Network-Constrained Multiperiod Auction for a Pool-Based Electricity Market," *IEEE Transactions on Power Systems*, vol. 17, no. 3, pp. 646–653, Aug. 2002.

[3] T. Overbye, X. Cheng, and Y. Sun, "A Comparison of the AC and DC Power Flow Model for LMP Calculations," in *37th Hawaii Int. Conf. Syst. Sci. (HICSS)*, Jan. 2006.

[4] B. Stott, J. Jardim, and O. Alsac, "DC Power Flow Revisited," *IEEE Transactions on Power Systems*, vol. 24, no. 3, pp. 1290–1300, Aug. 2009.

[5] S. Low, "Convex Relaxation of Optimal Power Flow–Part I: Formulations and Equivalence," *IEEE Transactions on Control of Network Systems*, vol. 1, no. 1, pp. 15–27, March 2014.

[6] J. Lavaei and S. Low, "Zero Duality Gap in Optimal Power Flow Problem," *IEEE Transactions on Power Systems*, vol. 27, no. 1, pp. 92–107, Feb. 2012.

[7] B. Lesieutre, D. Molzahn, A. Borden, and C. DeMarco, "Examining the Limits of the Application of Semidefinite Programming to Power Flow Problems," in *49th Annu. Allerton Conf. Commun., Control, Comput.*, Sept. 2011, pp. 1492–1499.

[8] D. Molzahn, B. Lesieutre, and C. DeMarco, "Investigation of Non-Zero Duality Gap Solutions to a Semidefinite Relaxation of the Optimal Power Flow Problem," in *47th Hawaii Int. Conf. Syst. Sci. (HICSS)*, 6-9 Jan. 2014.

[9] A. Wood, B. Wollenberg, and G. Sheble, *Power Generation, Operation and Control*, 3rd ed. John Wiley and Sons, Inc., 2013.

[10] F. Bouffard and F. F. Galiana, "Stochastic security for operations planning with signiffcant wind power generation," *IEEE Transactions on Power Systems*, vol. 23, no. 2, pp. 306–316, 2008.

[11] A. Papavasiliou, S. Oren, and R. ONeill, "Reserve requirements for wind power integration: A scenario-based stochastic programming framework," *IEEE Transactions on Power Systems*, vol. 26, no. 4, pp. 2197–2206, 2011.

[12] J. Morales, A. Conejo, and J. Perez-Ruiz, "Economic valuation of reserves in power systems with high penetration of wind power," *IEEE Transactions on Power Systems*, vol. 24, no. 2, pp. 900–910, 2009.

[13] M. Vrakopoulou, K. Margellos, J. Lygeros, and G. Andersson, "Probabilistic guarantees for the N-1 security of systems with wind power generation," in *Probabilistic Methods Applied to Power Systems Conference*, 2012.

[14] L. Roald, F. Oldewurtel, T. Krause, and G. Andersson, "Analytical Reformulation of Security Constrained Optimal Power Flow with Probabilistic Constraints," in *IEEE PowerTech Conference*, 2013.

[15] D. Bienstock, M. Chertkov, and S. Harnett, "Chance-constrained optimal power flow: Risk-aware network control under uncertainty," *SIAM Review*, vol. 56, no. 3, pp. 461–495, 2014.

[16] D. Bertsimas, E. Litvinov, X. Sun, J. Zhao, and T. Zheng, "Adaptive robust optimization for the security constrained unit commitment problem," *IEEE Transactions on Power Systems*, vol. 28, no. 1, pp. 52–62, 2013.

[17] G. Calafore and M. C. Campi, "The scenario approach to robust control design," *IEEE Transactions on Automatic Control*, vol. 51, no. 5, pp. 742–753, 2006.

[18] T. Alamo, R. Tempo, and A. Luque, "On the sample complexity of randomized approaches to the analysis and design under uncertainty," *Proceedings of the American Control Conference*, 2010.

[19] K. Margellos, P. Goulart, and J. Lygeros, "On the road between robust optimization and the scenario approach for chance constrained optimization problems," *IEEE Transactions on Automatic Control*, vol. 59, no. 8, pp. 2258–2263, 2014.

[20] M. Vrakopoulou, M. Katsampani, K. Margellos, J. Lygeros, and G. Andersson, "Probabilistic security-constrained AC optimal power flow," in *IEEE PowerTech Conference*, 2013.

[21] M. Campi, S. Garatti, and F. Ramponi, "Non-convex scenario optimization with application to system identification," in *54th IEEE Conference on Decision and Control*, 2015.

[22] J. F. Marley, M. Vrakopoulou, and I. A. Hiskens, "An AC-QP optimal power flow algorithm considering wind forecast uncertainty," in *IEEE Innovative Smart Grid Technologies - Asia (ISGT-Asia)*, 2016.

[23] J. Marley, D. Molzahn, and I. Hiskens, "Solving multiperiod OPF problems using an AC-QP algorithm initialized with an SOCP relaxation," *IEEE Transactions on Power Systems*, 2017, to appear.

[24] A. M. Giacomoni and B. F. Wollenberg, "Linear Programming Optimal Power Flow Utilizing a Trust Region Method," in *North Amer. Power Symp.*, 2010.

[25] K. Margellos, M. Prandini, and J. Lygeros, "On the connection between compression learning and scenario based single-stage and cascading optimization problems," *IEEE Transactions on Automatic Control*, vol. 60, no. 10, pp. 2716–2721, 2015.

[26] R. Zimmerman, C. Murillo-Sánchez, and R. Thomas, "MATPOWER: Steady-State Operations, Planning, and Analysis Tools for Power Systems Research and Education," *IEEE Trans. Power Syst.*, vol. 26, no. 1, pp. 12–19, 2011.